Single-Molecule Devices

DOI: 10.1002/ange.201308398

Single-Molecule Sensing of Environmental pH—an STM Break Junction and NEGF-DFT Approach**

Zhihai Li, Manuel Smeu, Sepideh Afsari, Yangjun Xing, Mark A. Ratner, and Eric Borguet**

Abstract: *Sensors play a significant role in the detection of toxic species and explosives, and in the remote control of chemical processes. In this work, we report a single-molecule-based pH switch/sensor that exploits the sensitivity of dye molecules to environmental pH to build metal–molecule–metal (m-M-m) devices using the scanning tunneling microscopy (STM) break junction technique. Dyes undergo pH-induced electronic modulation due to reversible structural transformation between a conjugated and a nonconjugated form, resulting in a change in the HOMO–LUMO gap. The dye-mediated m-M-m devices react to environmental pH with a high on/off ratio (≈100:1) of device conductivity. Density functional theory (DFT) calculations, carried out under the non-equilibrium Green's function (NEGF) framework, model charge transport through these molecules in the two possible forms and confirm that the HOMO–LUMO gap of dyes is nearly twice as large in the nonconjugated form as in the conjugated form.*

The miniaturization of electronic components involves a continued shrinkage in terms of device size and increased sensitivity of the sensing unit. The ultimate limit would be at the single-molecule level.[1,2] To build a single-molecule pH-based electrical sensor requires that we wire a single tailored molecule into a circuit, in other words "soldering" the molecule to at least two electrodes so that electrons can flow through such a single-molecule circuit when a voltage is applied between the two electrodes.[3–7] In addition, the electrical properties of the central component (the molecule) must be sensitive to environmental pH. For example, the conductance of the sensing molecule must vary when the surrounding pH changes.

In this work, we explore the concept of the single-molecule pH electrical sensor by deliberately choosing two dyes (Figure 1), malachite green (MG) and pararosaniline (PA), as molecular sensing units. As pH indicators, dyes show distinctive color differences when the pH of the solution changes, indicating an electronic perturbation often caused by pH-induced structural changes in the molecules. For example, in the present study, MG is in a conjugated form in neutral or slightly acidic solution, showing a blue–green color (Figure 1B). However, in basic solution (pH > 13) MG loses its internal conjugation and becomes colorless; in other words,

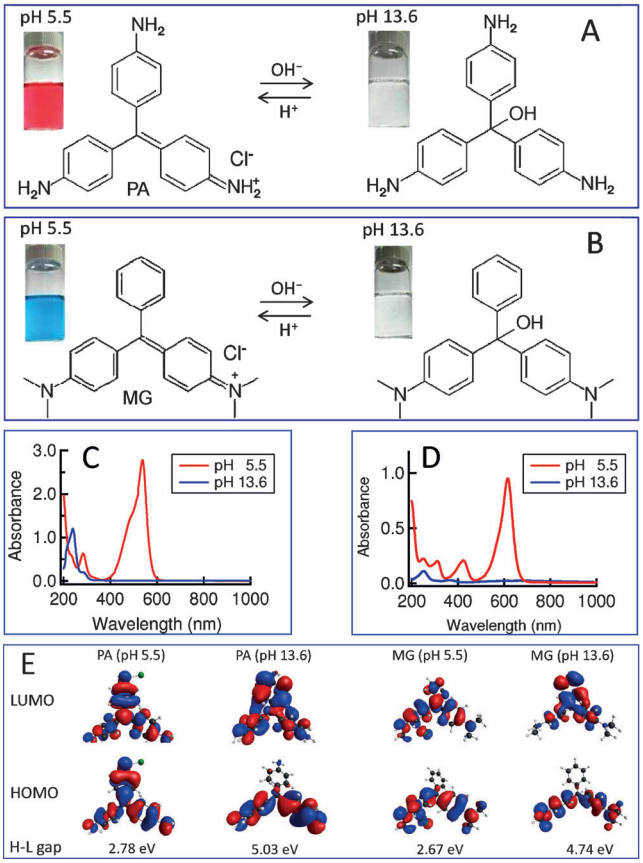

Figure 1. Molecular structures of pararosaniline (PA, panel A) and malachite green (MG, panel B) at different pH values. At pH 5.5, both PA and MG are in the conjugated form; in basic solution (pH 13.6), PA and MG lose conjugation by the introduction of an OH group to the central carbon atom which is thereby converted from sp^2 to sp^3 hybridization. Photographs show the dramatic change of solution color of PA and MG at different pH. C,D) UV/Vis spectra of PA (C) and MG (D). E) The frontier molecular orbitals for these molecules. The HOMO–LUMO (H-L) gap is also listed for each molecule.

[*] Dr. Z. Li, S. Afsari, Dr. Y. Xing, Prof. E. Borguet
Department of Chemistry, Temple University
1901 North 13th Street, Philadelphia, PA 19122 (USA)
E-mail: eborguet@temple.edu
Dr. M. Smeu, Prof. M. A. Ratner
Department of Chemistry, Northwestern University
Evanston, IL 60208 (USA)
E-mail: ratner@northwestern.edu

[**] We thank Vu Nguyen and Navin Rao for help with measuring the UV/Vis spectra of the dye molecules. We thank the National Science Foundation (CHE 0809838 to E.B., CHE-1058896 to M.S., CHE-1058896 to M.A.R.) and the FRQNT (M.S.) for financial support. STM = scanning tunneling microscopy, NEGF-DFT = density functional theory calculations carried out under framework of the non-equilibrium Green's function.

Supporting information for this article is available on the WWW under http://dx.doi.org/10.1002/anie.201308398.

MG molecules undergo a pH-induced electronic modulation due to a reversible structural transformation between a conjugated and a nonconjugated form (Figure 1). Such a pH-triggered structural modification shifts the HOMO–LUMO gap, indicated by the color change of the solution and perturbations of the absorption peaks in the UV/Vis spectra (Figure 1 D). Density functional theory (DFT) calculations on these molecules reveal that the HOMO–LUMO gap changes from 2.7 to 4.7 eV for MG and from 2.8 to 5.0 eV for PA when going from the conjugated to the nonconjugated form (Figure 1 E). Also, for both molecules the LUMO energy increases significantly (see Table 1). The pH-induced changes in the molecular structure and electronic properties of dyes suggest that dye-mediated junction devices present a unique opportunity to fabricate single-molecule pH sensors based on their electrical switching function.

First, we carried out single-molecule conductance (SMC) break junction experiments using (amine-terminated) PA in a weakly acidic solution (pH 5.5) where the molecule is in a conjugated form and has a wine-red color (Figure 1 A). The UV/Vis absorption spectrum shows a strong peak at 520 nm (red curve in Figure 1 C). When the solution pH is changed from 5.5 to 13.6, the orbital hybridization of the central carbon atom changes from sp^2 to sp^3, and the molecule loses the conjugation between the aniline rings, resulting in the disappearance of the 520 nm peak and the appearance of new peaks around 250 nm (Figure 1 C). The large absorption peak shift due to the pH change suggests a dramatic increase of the molecular HOMO–LUMO band gap, as confirmed by the DFT calculations (Figure 1 E).

The procedures for SMC experiments are described in the Supporting Information and elsewhere.[8–10] Several typical stepped current–distance traces are shown in Figure 2 B (inset, blue) for PA measured at pH 5.5. The presence of steps in the current–distance traces corresponds to the formation of molecular junctions,[4,11] in which the electrical current (I) through the junction (molecular conductor) remains approximately constant as the electrode separation increases ($I = G_m V_b$, where G_m is the molecular conductance and V_b is the voltage bias between the two electrodes). To obtain the junction resistance of the m-M-m device, we construct logarithmic current histograms (Figure 2 B) using all the current–distance traces without data selection. The all-data point histogram for PA in Figure 2 B was constructed from 3000 recorded current–distance traces and shows a current peak around 2.7 nA, which corresponds to the SMC of 67.5 nS (8.7×10^{-4} G_o), for $V_{bias} = 0.04$ V. The SMC values measured from different experiments on different days were averaged (see Table 1).

We also carried out SMC experiments on MG, which shares a similar core structure with PA but whose anchoring groups are $N(CH_3)_2$ instead of the NH_3 groups in PA. The current histogram (Figure 2 C) shows a clear current maximum and the average SMC value for MG at pH 5.5 solution is (65.6 ± 12.8) nS, comparable with the conductance of PA [(71.6 ± 8.6) nS, Table 1]. As MG and PA have the same core structure and different anchoring groups for connection to the gold electrode, the comparable conductance for the two molecules suggests that these two types of anchoring groups have similar "contact resistance" (for details see the Supporting Information).

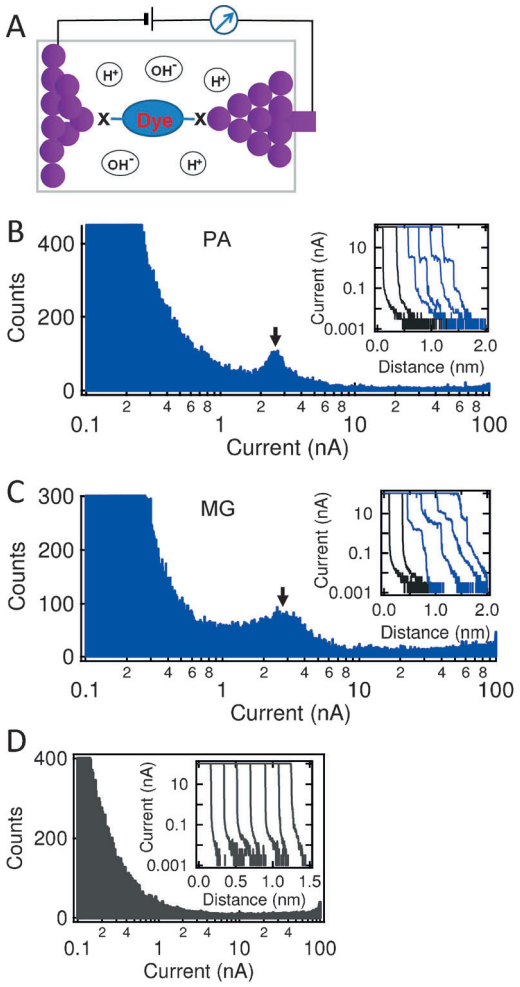

Figure 2. A) Representation of an STM break junction single-molecule pH electrical sensor. B) All-data point current histograms constructed from 3000 current–distance traces for PA, and C) from 2000 current–distance traces for MG, measured in pH 5.5 solution at $V_{bias} = 0.04$ V (insets show stepped traces. D) Current histogram constructed from 2000 current–distance traces measured in pH 5.5 solution, without adding dye, as a control. Typical individual current–distance traces in the control experiment are shown in the inset.

Table 1: Summary of SMC of PA and MG in acidic and basic pH environments and several other quantities obtained from calculations.

	pH	SMC [nS]	HOMO [eV]	LUMO [eV]	HOMO–LUMO gap [eV]
PA	5.5	71.6 ± 8.6	−5.61	−2.83	2.78
MG	5.5	65.6 ± 12.8	−5.25	−2.59	2.67
PA	13.6	0.73 ± 0.10	−4.95	0.08	5.03
MG	13.6	0.72 ± 0.10	−4.71	0.03	4.74

Control experiments were carried out under exactly the same experimental conditions but without added dye molecules. The resulting individual traces do not show evidence of the characteristic current steps and the histogram shows no discernable current peaks (Figure 2 D).

Break junction experiments for PA and MG were also performed in basic solution (pH 13.6), in which the loss of conjugation makes PA and MG solutions colorless (Figure 1). The absence of absorption in the visible spectral range suggests a dramatic increase of the molecular HOMO–LUMO gap. The current histogram for PA (Figure 3A) clearly shows a current maximum at 0.07 nA. The mean SMC value, 0.73 nS ±0.10 nS for PA at pH 13.6 solution, determined by averaging histogram current peak values from different experiments, is about two orders of magnitude smaller than in acidic solution, indicating a switching and environmental-sensing behavior caused by a pH-induced change of electronic properties of the dyes. Similarly, the SMC for MG in basic solution (pH 13.6) is determined to be (0.72 ± 0.10) nS, almost two orders of magnitude lower than in acidic solution (65.6 nS), which further confirms the conductance switching triggered by the conjugation and electronic changes of the sensing units (dyes). We modulated the conductance by performing experiments in solutions of the two dyes at different pH showing the robust and reversible conductance change between the "on" (high conductance) and "off" (low conductance) states (Figure 3E,F).

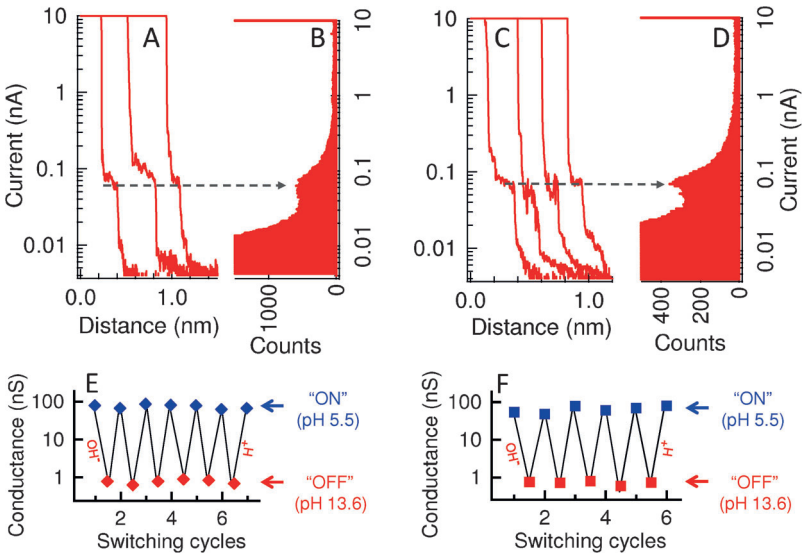

Figure 3. A,C) Logarithmic plotting of sample individual current–distance traces for PA (A) and MG (C) measured in pH 13.6 solution at $V_{bias} = 0.1$ V. B,D) All-data point current histograms constructed from 5000 current–distance traces without data selection for PA (B) and MG (D). E,F) Sequential cycles of pH-induced conductance modulation of PA (E) and MG (F) between "on" and "off" states.

Previous work investigated the conductance switching effects on single molecules through electrochemical gating,[11–19] photo switching,[20–27] and mechanically controlling molecular configurations.[28] The few prior reports of the modulation of molecular conductance through changes in the solution pH show either a small switching effect (on/off ratio of about 2),[29] or the detection of only one state at one pH, presumably the high conductance state, while the conductance value of the second state was not detected, either because a junction could not be formed or the conductance was too low.[30,31] In this work, we detected both the on and off states, revealing an on/off ratio of roughly 100:1.

To confirm that the observed conductance "on/off" switch is triggered by the response of the sensing unit (dye molecules) to solution pH through a conjugation change, we carried out SMC experiments at different pH values using octanedithiol, whose conjugation and electronic structure are not affected by solution pH. The results (see Figure S3 in the Supporting Information) show that the SMC of octanedithiol remains approximately the same when the solution pH was changed from neutral to acidic and/or basic, supporting our assertion that pH-induced structural and electronic changes are essential for the observed single-molecule sensing behavior.

To understand the pH-sensitive switching mechanism, electron transport calculations were carried out for these molecules bridging Au electrodes. Using the non-equilibrium Green's function (NEGF) formalism with density functional theory (DFT), we calculated the transmission spectra for these systems, which represent the probability that an electron with a given energy will transmit through the molecule between the electrodes (see Figure 4). This technique has been discussed in detail elsewhere,[32–34] and a brief summary of our approach is provided in the Supporting Information. The two-probe structures for the two molecules at pH 5.5 and 13.6 are shown in Figure 4.

The transmission spectra for the four systems (top: PA, bottom: MG, black: pH 5.5, red: pH 13.6) are also shown in Figure 4. The key result is that the transmission through either PA or MG is more than two orders of magnitude higher through the molecule at pH 5.5 than through the molecule at pH 13.6, in agreement with the experimentally measured conductance. It should be pointed out that we cannot make a direct comparison of the calculated transmission and the experimentally measured SMC. This is because computational cost made it necessary to use electrodes of finite cross section, resulting in a different E_F and electrode–molecule coupling than in the experiment. Therefore, we can only compare the relative values (ratio) for a given molecule at pH 5.5 and 13.6. Indeed the black plot is overall higher than the red plot at most energies for both molecules. There is one exception for PA at pH 5.5, where there is a dip in transmission near −1.2 eV. This is an interference feature due to the particular structure and symmetry of this molecule.

The reason that the overall transmission is higher at pH 5.5 is because there is a transmission peak just above E_F, which corresponds to electrons passing through the LUMO of the molecule (see the Supporting Information for linear-scale transmission spectra and scattering state analysis). At pH 13.6, the LUMO is much higher in energy, resulting in the transmission peaks near 2 eV relative to E_F in Figure 4 (red plots).

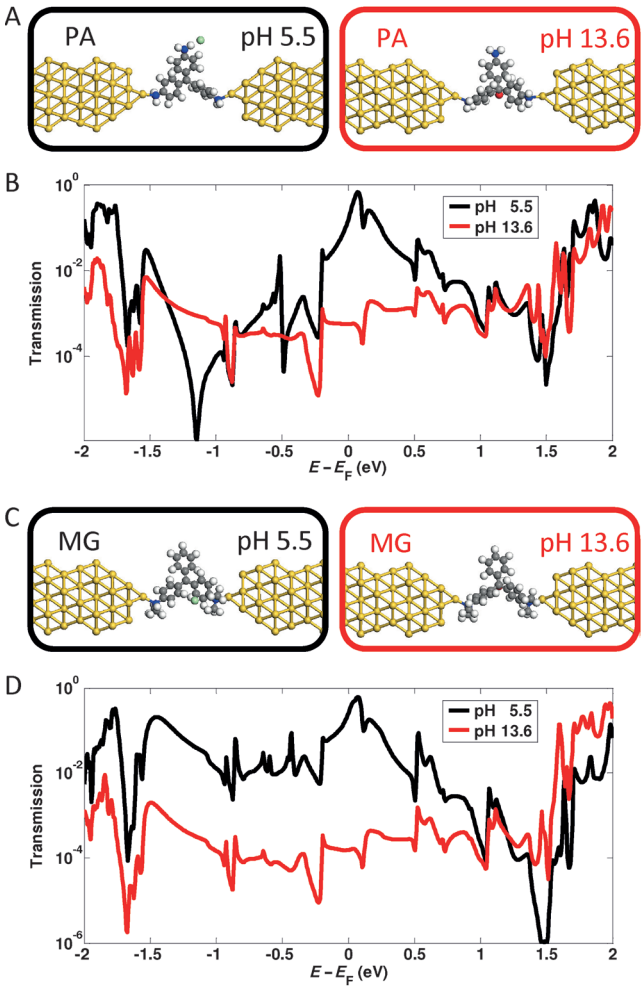

Figure 4. A,C) The two-probe structures used in the electron transport calculations for PA and MG at the two pH values. The main difference is that at pH 5.5, the central carbon atom is sp^2 hybridized, while at pH 13.6 the central carbon is sp^3 hybridized as an OH group binds to it. B,D) Transmission spectra for PA (B) ande MG (D) under different pH conditions ($E_F = -3.35$ eV).

In summary, we have demonstrated single-molecule pH-sensing behavior using a new type of electrical switch based on the pH-induced conjugation and electronic change of dye molecules. The m-M-m devices fabricated can be reversibly switched between the on and off states by means of the pH of the media solution at an on/off conductance ratio of about two orders of magnitude. The present work not only shows that solution pH can be used as a simple parameter to trigger the conductance change, but also illustrates that -$N(CH_3)_2$ can be used as an anchoring group to bind to gold electrodes. DFT calculations confirmed the increase in the HOMO–LUMO gap when the hybridization of the central C atom changes from sp^2 to sp^3, which is driven by the solution pH. Electron transport calculations agree with experiment showing a difference of roughly two orders of magnitude between the conductance of the molecule at these different pH levels, which is due to the shift of the LUMO level.

Received: September 25, 2013
Published online: December 11, 2013

Keywords: density functional calculations · dyes/pigments · molecular electronics · pH sensors · sensing · single-molecule devices

[1] J. Janata, M. Josowicz, D. M. Devaney, *Anal. Chem.* **1994**, *66*, R207 – R208.
[2] H. Craighead, *Nature* **2006**, *442*, 387 – 393.
[3] S. H. Choi, B. Kim, C. D. Frisbie, *Science* **2008**, *320*, 1482 – 1486.
[4] B. Q. Xu, N. J. Tao, *Science* **2003**, *301*, 1221 – 1223.
[5] L. Venkataraman, J. E. Klare, C. Nuckolls, M. S. Hybertsen, M. L. Steigerwald, *Nature* **2006**, *442*, 904 – 907.
[6] A. Nitzan, M. A. Ratner, *Science* **2003**, *300*, 1384 – 1389.
[7] M. L. Perrin, F. Prins, C. A. Martin, A. J. Shaikh, R. Eelkema, J. H. van Esch, T. Briza, R. Kaplanek, V. Kral, J. M. van Ruitenbeek, H. S. J. van der Zant, D. Dulic, *Angew. Chem.* **2011**, *123*, 11419 – 11422; *Angew. Chem. Int. Ed.* **2011**, *50*, 11223 – 11226.
[8] Z. Li, E. Borguet, *J. Am. Chem. Soc.* **2012**, *134*, 63 – 66.
[9] Z. Li, T. H. Park, J. Rawson, M. J. Therien, E. Borguet, *Nano Lett.* **2012**, *12*, 2722 – 2727.
[10] Z. Li, M. Smeu, M. A. Ratner, E. Borguet, *J. Phys. Chem. C* **2013**, *117*, 14890 – 14898.
[11] Z. Li, B. Han, G. Meszaros, I. Pobelov, T. Wandlowski, A. Blaszczyk, M. Mayor, *Faraday Discuss.* **2006**, *131*, 121 – 143.
[12] I. Diez-Perez, Z. H. Li, J. Hihath, J. H. Li, C. Y. Zhang, X. M. Yang, L. Zang, Y. J. Dai, X. L. Feng, K. Muellen, N. J. Tao, *Nat. Commun.* **2010**, *1*, 1.
[13] B. Q. Xu, X. Y. Xiao, X. M. Yang, L. Zang, N. J. Tao, *J. Am. Chem. Soc.* **2005**, *127*, 2386 – 2387.
[14] W. Haiss, H. van Zalinge, S. J. Higgins, D. Bethell, H. Hobenreich, D. J. Schiffrin, R. J. Nichols, *J. Am. Chem. Soc.* **2003**, *125*, 15294 – 15295.
[15] N. J. Kay, S. J. Higgins, J. O. Jeppesen, E. Leary, J. Lycoops, J. Ulstrup, R. J. Nichols, *J. Am. Chem. Soc.* **2012**, *134*, 16817 – 16826.
[16] E. Leary, S. J. Higgins, H. van Zalinge, W. Haiss, R. J. Nichols, S. Nygaard, J. O. Jeppesen, J. Ulstrup, *J. Am. Chem. Soc.* **2008**, *130*, 12204 – 12205.
[17] Z. H. Li, Y. Q. Liu, S. F. L. Mertens, I. V. Pobelov, T. Wandlowski, *J. Am. Chem. Soc.* **2010**, *132*, 8187 – 8193.
[18] X. S. Zhou, L. Liu, P. Fortgang, A. S. Lefevre, A. Serra-Muns, N. Raouafi, C. Amatore, B. W. Mao, E. Maisonhaute, B. Schollhorn, *J. Am. Chem. Soc.* **2011**, *133*, 7509 – 7516.
[19] N. Darwish, I. Diez-Perez, P. Da Silva, N. J. Tao, J. J. Gooding, M. N. Paddon-Row, *Angew. Chem.* **2012**, *124*, 3257 – 3260; *Angew. Chem. Int. Ed.* **2012**, *51*, 3203 – 3206.
[20] S. J. van der Molen, P. Liljeroth, *J. Phys. Condens. Matter* **2010**, *22*, 133001.
[21] N. Katsonis, T. Kudernac, M. Walko, S. J. van der Molen, B. J. van Wees, B. L. Feringa, *Adv. Mater.* **2006**, *18*, 1397 – 1400.
[22] M. Kiguchi, K. Tahara, Y. Takahashi, K. Hasui, Y. Tobe, *Chem. Lett.* **2010**, *39*, 788 – 789.
[23] S. Lara-Avila, A. V. Danilov, S. E. Kubatkin, S. L. Broman, C. R. Parker, M. B. Nielsen, *J. Phys. Chem. C* **2011**, *115*, 18372 – 18377.
[24] S. Martin, W. Haiss, S. J. Higgins, R. J. Nichols, *Nano Lett.* **2010**, *10*, 2019 – 2023.
[25] E. S. Tam, J. J. Parks, W. W. Shum, Y. W. Zhong, M. B. Santiago-Berrios, X. Zheng, W. T. Yang, G. K. L. Chan, H. D. Abruna, D. C. Ralph, *ACS Nano* **2011**, *5*, 5115 – 5123.
[26] K. Uchida, Y. Yamanoi, T. Yonezawa, H. Nishihara, *J. Am. Chem. Soc.* **2011**, *133*, 9239 – 9241.

[27] D. Roldan, V. Kaliginedi, S. Cobo, V. Kolivoska, C. Bucher, W. Hong, G. Royal, T. Wandlowski, *J. Am. Chem. Soc.* **2013**, *135*, 5974 – 5977.
[28] S. Y. Quek, M. Kamenetska, M. L. Steigerwald, H. J. Choi, S. G. Louie, M. S. Hybertsen, J. B. Neaton, L. Venkataraman, *Nat. Nanotechnol.* **2009**, *4*, 230 – 234.
[29] X. Y. Xiao, B. Q. Xu, N. J. Tao, *J. Am. Chem. Soc.* **2004**, *126*, 5370 – 5371.
[30] L. Scullion, T. Doneux, L. Bouffier, D. G. Fernig, S. J. Higgins, D. Bethell, R. J. Nichols, *J. Phys. Chem. C* **2011**, *115*, 8361 – 8368.
[31] Y. Cao, S. Dong, S. Liu, Z. Liu, X. Guo, *Angew. Chem.* **2013**, *125*, 3998 – 4002; *Angew. Chem. Int. Ed.* **2013**, *52*, 3906 – 3910.
[32] M. Smeu, R. Wolkow, H. Guo, *Theor. Chem. Acc.* **2012**, *131*, 1 – 8.
[33] D. Waldron, P. Haney, B. Larade, A. MacDonald, H. Guo, *Phys. Rev. Lett.* **2006**, *96*, 166804.
[34] J. Taylor, H. Guo, J. Wang, *Phys. Rev. B* **2001**, *63*, 121104.

